Nat Hazards (2011) 57:617–642
DOI 10.1007/s11069-010-9535-4

ORIGINAL PAPER

Coupling between internal and surface waves

Walter Craig · Philippe Guyenne · Catherine Sulem

Received: 16 December 2009 / Accepted: 30 March 2010 / Published online: 7 May 2010

Abstract In a fluid system in which two immiscible layers are separated by a sharp free interface, there can be strong coupling between large amplitude nonlinear waves on the interface and waves in the overlying free surface. We study the regime where long waves propagate in the interfacial mode, which are coupled to a modulational regime for the free-surface mode. This is a system of Boussinesq equations for the internal mode, coupled to the linear Schrödinger equations for wave propagation on the free surface, and respectively a version of the Korteweg-de Vries equation for the internal mode in case of unidirectional motions. The perturbation methods are based on the Hamiltonian formulation for the original system of irrotational Euler's equations, as described in (Benjamin and Bridges, J Fluid Mech 333:301–325, 1997, Craig et al., Comm Pure Appl Math 58:1587–1641, 2005a, Zakharov, J Appl Mech Tech Phys 9:190–194, 1968), using the perturbation theory for the modulational regime that is given in (Craig et al. to appear). We focus in particular on the situation in which the internal wave gives rise to localized bound states for the Schrödinger equation, which are interpreted as surface wave patterns that give a characteristic signature of the presence of an internal wave soliton. We also comment on the discrepancies between the free interface-free surface cases and the approximation of the upper boundary condition by a rigid lid.

Keywords Hamiltonian systems · Internal waves · Surface waves

Mathematics Subject Classification (2000) 37K05 · 76B07 · 76B15 · 76B55

W. Craig (✉)
Department of Mathematics, McMaster University, Hamilton, ON L8S 4K1, Canada
e-mail: craig@math.mcmaster.ca

P. Guyenne
Department of Mathematical Sciences, University of Delaware, Newark, DE 19716, USA
e-mail: guyenne@math.udel.edu

C. Sulem
Department of Mathematics, University of Toronto, Toronto, ON M5S 3G3, Canada
e-mail: sulem@math.toronto.edu

1 Introduction

In the situation in which a fluid domain, such as the sea, consists of essentially two immiscible layers separated by a sharp interface such as a thermocline or a pycnocline of differential salinity, very large amplitude and long wavelength nonlinear waves can be produced in the interface and can propagate over large distances. Despite the fact that internal waves of a variety of types are commonly generated in the world's oceans, it is only surprisingly recently that they have been observed and accurately measured. Several of the earliest observations are most striking, consisting of long brightly shining strips of many kilometers in extent in the Andaman Sea, visible through the effect of the reflection at an oblique angle of the setting sun, and photographed from the Space Shuttle (see the Office of Naval Research report, Global Ocean Associates 2002; Osborne and Burch 1980). The changes in reflectance of the wave pattern on the ocean surface are due to the presence of a roughness, akin to a tidal rip, the result of a coupling between internal waves and free-surface waves, which is the subject of this paper.

In our analysis, we derive model equations for interfacial and surface waves, which describe the evolution of large amplitude nonlinear motions of an interface between two internal fluid layers, and its coupling with the motion of an overlying free surface. The perturbation methods that we use are based on the Hamiltonian formulation of the problem, and are extensions of those that are developed in (Craig and Groves 1994, Craig et al. 2010) for the free-surface problem. While many studies of internal waves are based on approximations which impose a rigid lid boundary condition on the upper boundary of the fluid, it is important in the description of the interface-surface coupling to retain the full free-surface conditions. In this situation and in the regime of linear analysis, there are two normal modes, one for the displacements of the free-surface and the other for the interfacial motions. Denote their respective dispersion relations by $\omega_1(k)$ and $\omega(k)$. Since the group velocity of the free-surface mode $c_0^+(k) := \partial_k\omega_1(k)$ is always larger than the group velocity $c_0^-(k) := \partial_k\omega(k)$ of the interfacial mode (Craig et al. 2004, 2005a), it is natural when considering the long-wave regime for the interface, to study the free-surface as described in a modulational regime. The carrier frequency k_0 for these modulational waves is such that their group velocity satisfies the resonance condition $\partial_k\omega_1(k_0) = c_0^-(0)$, the latter quantity being the propagation velocity of the long interfacial waves. Furthermore, the most relevant problems of the motion of ocean waves are expected to satisfy $\varepsilon_1 \ll \varepsilon^2$, where ε_1 is a typical amplitude of the surface waves, while ε^2 is the typical amplitude of internal wave motions. We find for small $\varepsilon, \varepsilon_1$ that the internal waves will satisfy asymptotically a Boussinesq equation, or its unidirectional version, the Korteweg-de Vries (KdV) equation. The surface waves are then driven by the motions of the interface, solving a transport equation at the group velocity $\partial_k\omega_1(k_0)$, with their envelope modulated by a linear Schrödinger equation. For some important cases of solitary wave solutions of the internal wave mode, the linear Schrödinger equation exhibits bound states, which are interpreted physically as a characteristic signature of the presence of internal waves.

The study of the long-wave regime for internal waves was initiated in the two papers of Benjamin (1966, 1967), who studied the case of rigid lid upper boundary conditions. He derived the well-known criterion for the presence of positive vs. negative solitary wave solutions in the fluid interface, using the KdV model equations. The article of Gear and Grimshaw (1984) addressed the problem with the more realistic free-surface boundary conditions imposed on the upper free-surface. In this analysis, however, they assumed that the evolution of the interface and the free surface are both in the long-wave regime. Because of the strict inequality $c_0^-(0) < c_0^+(0)$ mentioned earlier, the resonance condition is

never satisfied, localized long-wave regime disturbances of the free surface will always move faster than similarly localized disturbances in the interface, and the two solutions will decouple. The most comparable work to our present analysis is that of Hashizume (1980), who studies precisely the regime of a coupled long-wave regime in an interface with a modulational regime for the upper free surface of the fluid body. He uses a classical multiple scales perturbation method, and, in contrast to our focus of interest, is interested in the case of large amplitude nonlinear surface displacements coupled to large amplitude motions of the interface. More recently, there have been a number of articles on this problem, from a variety of points of view. Namely, Benjamin and Bridges (1997) reassessed the theory in Benjamin's previous work, using as a starting point the formulation of the interface with rigid lid problem as a system of Hamiltonian partial differential equations. Choi and Camassa (1999) studied large amplitude interfacial waves, again with rigid lid upper boundary conditions. Dias and Ilichev (2001) modeled both classical and generalized interfacial solitary waves beneath a linear free surface, and Parau and Dias (2001) numerically computed such solutions. Finally, Craig et al. (2004, 2005a) consider both the cases of rigid lid and free surface upper boundary conditions in the long-wave scaling regime. They derive a Hamiltonian formulation for the equations of motion in both cases, and they analyse a number of aspects of the two problems for which the rigid lid assumption is and is not a good approximation for the problem of an upper free surface. The work in the present paper considers the situation in which the surface mode appears in a modulational regime, whereas the internal mode remains in the long-wave regime. It represents a continuation of the previous analysis of Craig et al. (2004, 2005a).

There in addition has been a continuing interest over many years in the rigorous mathematical analysis of the problem of internal waves. One earlier work is the paper of Peters and Stoker (1960) on the existence of solitary waves in internal layers, with free surface boundary conditions on the upper fluid boundary. Bona et al. (2008) studied the initial value problem for the problem of a fluid interface with rigid lid upper boundary conditions, deriving in a mathematically rigorous manner the validity of various of the long wave asymptotic models for internal waves. The paper of Colin and Lannes (2001) addresses a problem in nonlinear waves which involves the coupling of long and short waves, in a system which is in some ways similar to the present case at hand. Duchêne (2009) studies the more complex problem of rigorous justification of asymptotic models for coupled free-surface/free-interface evolution in the case of an interface and an upper free boundary to the fluid domain.

In the present paper, we start our analysis with the incompressible irrotational Euler equations of motion for a body of fluid consisting of two immiscible layers separated by a dynamical interface. The bottom of the fluid domain is fixed, and as for the upper fluid boundary, we consider principally the case of free surface boundary conditions, keeping rigid lid conditions for contrast and comparison. In Sect. 2, we derive the Hamiltonian structure for this problem, on which our asymptotic analysis is based. This is an extension of the original ideas of Zakharov (1968) for the Hamiltonian formulation of the free surface water waves problem, which was then revisited in (Craig and Sulem 1993). The case of a rigid lid upper boundary condition was shown to be a Hamiltonian partial differential equation in (Benjamin and Bridges 1997), with a similar Hamiltonian given in Craig and Groves (2000). Since the kinetic energy is expressed in terms of the Dirichlet integrals for the two fluid domains, in Sect. 3 we provide a detailed asymptotic analysis of the Dirichlet-Neumann operators for the different fluid domains and interfaces. This has previously been worked out in (Craig et al. 2004, 2005a). In Sect. 4, we perform a normal mode analysis of the linearized equations for the free interface-free surface system, thus deriving the two

dispersion relations for the problem. These are compared with the case of rigid lid upper boundary conditions, for which there is only one internal mode. Finally, in Sect. 5, we perform the nonlinear long wave regime analysis to derive the model equations for the interface in the presence of the upper free surface. This is based on a general scaling approach that was introduced in (Craig and Groves 1994) and used effectively for the internal wave-free surface problem in (Craig et al. 2005a). We find that the internal mode solves asymptotically a KdV equation, while in the proper frame of reference the surface wave mode solves a linear Schrödinger equation. We discuss a criterion for the presence of bound states of this system, and the surface wave patterns that are generated. Again, important features such as the relative strengths of nonlinear to dispersive effects are compared to those for the case of the rigid lid.

2 Formulation of the problem

2.1 Equations of motion

The fluid domain is the region consisting of the points (x, y) such that $x \in \mathbb{R}, -h < y < h_1 + \eta_1(x,t)$, and it is divided into two regions $S(t;\eta) = \{(x,y) : x \in \mathbb{R}, -h < y < \eta(x,t)\}$ and $S_1(t;\eta,\eta_1) = \{(x,y) : x \in \mathbb{R}, \eta(x,t) < y < h_1 + \eta_1(x,t)\}$ by the interface $\{y = \eta(x, t)\}$. The two regions are occupied by two immiscible fluids, with ρ the density of the lower fluid and ρ_1 the density of the upper fluid. The system is in a stable configuration, in that $\rho > \rho_1$ (Fig. 1). In such a configuration, the fluid motion is assumed to be potential flow, namely in Eulerian coordinates the velocity is given by a potential in each fluid region, $\mathbf{u}(x, y, t) = \nabla\varphi(x, y, t)$ in $S(t;\eta)$, and $\mathbf{u}_1(x, y, t) = \nabla\varphi_1(x, y, t)$ in $S_1(t;\eta, \eta_1)$, where the two potential functions satisfy

$$\begin{aligned} \Delta\varphi &= 0, \quad \text{in the domain } S(t;\eta) \\ \Delta\varphi_1 &= 0, \quad \text{in the domain } S_1(t;\eta,\eta_1) \end{aligned} . \tag{1}$$

The boundary conditions on the fixed bottom $\{y = -h\}$ of the lower fluid are that

$$\nabla\varphi \cdot N_0(x,-h) = -\partial_y\varphi(x,-h) = 0, \tag{2}$$

where N_0 is the exterior unit normal, enforcing that there is no fluid flux across the boundary.

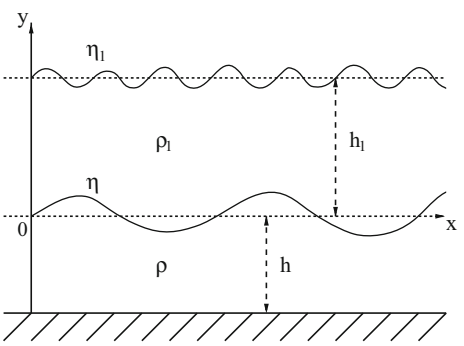

Fig. 1 Sketch of the physical domain which consists of two fluids of densities ρ and $\rho_1 < \rho$, and of depths h and h_1, separated by an interface of elevation η. The lower boundary of the domain is a uniform rigid bottom, while the upper boundary is a free surface of elevation η_1

On the interface $\{y = \eta(x, t)\}$, it is natural to impose three boundary conditions, two kinematic conditions which are essentially geometrical, and a physical condition of force balance. The kinematical conditions assume that there is no cavitation in the interface between the fluids, and therefore the function $\eta(x, t)$ whose graph defines the interface satisfies simultaneously

$$\partial_t \eta = \partial_y \varphi - \partial_x \eta \partial_x \varphi = \nabla \varphi \cdot N \left(1 + (\partial_x \eta)^2\right)^{1/2}, \tag{3}$$

where N is the unit exterior normal on the interface for the lower domain, and

$$\partial_t \eta = \partial_y \varphi_1 - \partial_x \eta \partial_x \varphi_1 = -\nabla \varphi_1 \cdot (-N) \left(1 + (\partial_x \eta)^2\right)^{1/2}. \tag{4}$$

The third boundary condition imposed on the interface is the Bernoulli condition, which states that

$$\rho \left(\partial_t \varphi + \frac{1}{2}|\nabla \varphi|^2 + g\eta\right) = \rho_1 \left(\partial_t \varphi_1 + \frac{1}{2}|\nabla \varphi_1|^2 + g\eta\right), \tag{5}$$

with g being the acceleration due to gravity.

Finally, on the top free surface $\{y = h_1 + \eta_1(x, t)\}$, the velocity potential φ_1 and the function η_1 satisfy a surface kinematic condition

$$\partial_t \eta_1 = \partial_y \varphi_1 - \partial_x \eta_1 \partial_x \varphi_1 = \nabla \varphi_1 \cdot N_1 \left(1 + (\partial_x \eta_1)^2\right)^{1/2}, \tag{6}$$

and a Bernoulli condition

$$\partial_t \varphi_1 + \frac{1}{2}|\nabla \varphi_1|^2 + g\eta_1 = 0. \tag{7}$$

The problem then is to describe the simultaneous evolution of the free surface $\{(x, h_1 + \eta_1(x, t))\}$ and the free interface $\{(x, \eta(x, t))\}$.

2.2 Canonical variables and Hamiltonian formulation

In this section, we identify the canonical variables and derive the form of the Hamiltonian functional following the lines of (Craig et al. 2005a). The system involves the coupled evolution of the free interface and a free surface lying over the upper fluid. This problem can be described in terms of a Lagrangian, which will depend upon both the deformations $\eta_1(x, t)$ of the free surface, as well as those of the free interface $\eta(x, t)$. The 'first principles' of mechanics can be cited in deriving the natural canonically conjugate variables for a Hamiltonian description of the problem and for a convenient expression of the Hamiltonian functional.

The kinetic energy is given as a weighted sum of the Dirichlet integrals of the two velocity potentials

$$K = \frac{1}{2}\int_{\mathbb{R}} \int_{-h}^{\eta(x)} \rho |\nabla \varphi(x, y)|^2 dy dx + \frac{1}{2}\int_{\mathbb{R}} \int_{\eta(x)}^{h_1 + \eta_1(x)} \rho_1 |\nabla \varphi_1(x, y)|^2 dy dx. \tag{8}$$

The potential energy is

$$V = \frac{1}{2}\int_{\mathbb{R}} g(\rho - \rho_1)\eta^2(x)dx + \frac{1}{2}\int_{\mathbb{R}} g\rho_1\left[(h_1 + \eta_1)^2(x) - h_1^2\right]dx. \tag{9}$$

The analogy with mechanics implies that the Lagrangian of the system is given by

$$L = K - V,$$

and in this analogy the configuration space variables are (η, η_1). We now express the Dirichlet integrals in terms of the boundary values for the two velocity potentials and the Dirichlet-Neumann operators for the two fluid domains. We define the quantities $\Phi(x) = \varphi(x, \eta(x)), \Phi_1(x) = \varphi_1(x, \eta(x))$, and $\Phi_2(x) = \varphi_1(x, h_1 + \eta_1(x))$ on the free surface. The Dirichlet-Neumann operator for the lower domain is

$$G(\eta)\Phi(x) \equiv (\nabla\varphi \cdot N)(x, \eta(x))\left(1 + (\partial_x\eta)^2\right)^{1/2}. \tag{10}$$

For the upper fluid domain $S_1(\eta, \eta_1)$, both $\Phi_1(x)$ and $\Phi_2(x)$ contribute to the exterior unit normal derivative of φ_1 on each boundary. That is, the Dirichlet-Neumann operator is a matrix operator which takes the form

$$\begin{pmatrix} G_{11} & G_{12} \\ G_{21} & G_{22} \end{pmatrix}\begin{pmatrix} \Phi_1(x) \\ \Phi_2(x) \end{pmatrix} \equiv \begin{pmatrix} -(\nabla\varphi_1 \cdot N)(x, \eta(x))\left(1 + (\partial_x\eta(x))^2\right)^{1/2} \\ (\nabla\varphi_1 \cdot N_1)(x, h_1 + \eta_1(x))\left(1 + (\partial_x\eta_1(x))^2\right)^{1/2} \end{pmatrix}. \tag{11}$$

Using Green's identities and expressing the normal derivatives of the velocity potentials on the boundaries in terms of Dirichlet-Neumann operators, the kinetic energy takes the form

$$K = \frac{1}{2}\int_{\mathbb{R}} \rho\Phi G(\eta)\Phi dx + \frac{1}{2}\int_{\mathbb{R}} \rho_1\begin{pmatrix} \Phi_1 \\ \Phi_2 \end{pmatrix}^{\top}\begin{pmatrix} G_{11} & G_{12} \\ G_{21} & G_{22} \end{pmatrix}\begin{pmatrix} \Phi_1 \\ \Phi_2 \end{pmatrix}dx. \tag{12}$$

To continue the analogy with Lagrangian mechanics, an expression for the tangent space variables $(\dot{\eta}, \dot{\eta}_1)$ is needed. In terms of the Dirichlet-Neumann operators (10, 11), the kinematic boundary condition (13) for $\Phi(x)$ is employed to define $\dot{\eta}$ as

$$\dot{\eta} = G(\eta)\Phi, \tag{13}$$

while (4) and (6) become

$$\begin{aligned} \dot{\eta} &= -(G_{11}\Phi_1 + G_{12}\Phi_2) \\ \dot{\eta}_1 &= G_{21}\Phi_1 + G_{22}\Phi_2. \end{aligned} \tag{14}$$

Using (13) and (14), we rewrite the kinetic energy in terms of the variables $(\eta, \eta_1, \dot{\eta}, \dot{\eta}_1)$, giving the following expression of the Lagrangian for the free interface-free surface problem,

$$\begin{aligned} L = &\frac{1}{2}\int_{\mathbb{R}} \rho\dot{\eta}G^{-1}(\eta)\dot{\eta}dx + \frac{1}{2}\int_{\mathbb{R}} \rho_1\begin{pmatrix} -\dot{\eta} \\ \dot{\eta}_1 \end{pmatrix}^{\top}\begin{pmatrix} G_{11} & G_{12} \\ G_{21} & G_{22} \end{pmatrix}^{-1}\begin{pmatrix} -\dot{\eta} \\ \dot{\eta}_1 \end{pmatrix}dx \\ &- \frac{1}{2}\int_{\mathbb{R}} g(\rho - \rho_1)\eta^2(x)dx - \frac{1}{2}\int_{\mathbb{R}} g\rho_1\left[(h_1 + \eta_1)^2(x) - h_1^2\right]dx. \end{aligned} \tag{15}$$

In these terms, we are able to deduce from 'first principles' the appropriate canonically conjugate variables for the problem (see Landau and Lifshitz 1960), namely the Legendre transform is stated as

$$\begin{pmatrix} \xi \\ \xi_1 \end{pmatrix} = \begin{pmatrix} \delta_{\dot\eta} L \\ \delta_{\dot\eta_1} L \end{pmatrix} = \rho \begin{pmatrix} G^{-1}(\eta)\dot\eta \\ 0 \end{pmatrix} + \rho_1 \begin{pmatrix} G_{11} & -G_{12} \\ -G_{21} & G_{22} \end{pmatrix}^{-1} \begin{pmatrix} \dot\eta \\ \dot\eta_1 \end{pmatrix} = \begin{pmatrix} \rho\Phi - \rho_1\Phi_1 \\ \rho_1\Phi_2 \end{pmatrix}. \tag{16}$$

The expression (16) also appears in (Benjamin and Bridges 1997). Using (16), the kinetic energy (12) has the form

$$K = \frac{1}{2}\int_{\mathbb{R}} \begin{pmatrix} \xi \\ \xi_1 \end{pmatrix}^{\top} \begin{pmatrix} \dot\eta \\ \dot\eta_1 \end{pmatrix} dx = \frac{1}{2}\int_{\mathbb{R}} \begin{pmatrix} \xi \\ \xi_1 \end{pmatrix}^{\top} \begin{pmatrix} -G_{11} & -G_{12} \\ G_{21} & G_{22} \end{pmatrix} \begin{pmatrix} \Phi_1 \\ \Phi_2 \end{pmatrix} dx. \tag{17}$$

Solving (13, 16) for (Φ, Φ_1, Φ_2) in terms of (ξ, ξ_1) and defining

$$B = \rho G_{11} + \rho_1 G(\eta),$$

we have

$$\Phi = B^{-1}(G_{11}\xi - G_{12}\xi_1) \tag{18}$$

$$\Phi_1 = B^{-1}\left(-G(\eta)\xi - \frac{\rho}{\rho_1} G_{12}\xi_1\right) \tag{19}$$

$$\rho_1\Phi_2 = \xi_1, \tag{20}$$

and (17) can be written as

$$K = \frac{1}{2}\int_{\mathbb{R}} \begin{pmatrix} \xi \\ \xi_1 \end{pmatrix}^{\top} \begin{pmatrix} G_{11}B^{-1}G(\eta) & -G(\eta)B^{-1}G_{12} \\ -G_{21}B^{-1}G(\eta) & \frac{1}{\rho_1}G_{22} - \frac{\rho}{\rho_1}G_{21}B^{-1}G_{12} \end{pmatrix} \begin{pmatrix} \xi \\ \xi_1 \end{pmatrix} dx. \tag{21}$$

The Hamiltonian for the free interface and free surface problem is $H = K + V$ where $K = K(\eta, \eta_1, \xi, \xi_1)$ is given by (21) and the potential energy $V = V(\eta, \eta_1)$ is simply expressed by (9).

In terms of the variables (η, ξ) and (η_1, ξ_1), the equations of motion take the canonical form

$$\partial_t \begin{pmatrix} \eta \\ \xi \\ \eta_1 \\ \xi_1 \end{pmatrix} \equiv J\nabla H = \begin{pmatrix} 0 & 1 & 0 & 0 \\ -1 & 0 & 0 & 0 \\ 0 & 0 & 0 & 1 \\ 0 & 0 & -1 & 0 \end{pmatrix} \begin{pmatrix} \delta_\eta H \\ \delta_\xi H \\ \delta_{\eta_1} H \\ \delta_{\xi_1} H \end{pmatrix}, \tag{22}$$

for the interface and free surface respectively.

3 Dirichlet-Neumann operators

The Dirichlet-Neumann operators for the lower fluid region $S(\eta)$ and the upper region $S(\eta, \eta_1)$ are analytic in their dependence on the domain (Coifman and Meyer 1985; Fazioli

and Nicholls 2008), as parametrized locally by the two functions $\eta(x)$ and $\eta_1(x)$. Their Taylor expanions in (η, η_1) about zero play a central role in the perturbation calculations of this paper. We derive expressions for the Taylor expansions of the Dirichlet-Neumann operators (10, 11) which are explicit in their dependence upon (η, η_1), and where the Taylor coefficients are recursively defined.

3.1 Lower fluid domain $S(\eta)$

For the lower fluid domain $S(\eta)$, a particular basis of harmonic functions is given by $\varphi_k(x, y) = a(k)e^{ky}e^{ikx} + b(k)e^{-ky}e^{ikx}$. Satisfying the bottom boundary conditions in (1), we find that $a(k) = e^{kh}/(e^{kh} + e^{-kh})$ and $b(k) = e^{-kh}/(e^{kh} + e^{-kh})$. Its boundary values on the free surface are

$$\Phi_k(x) = \varphi_k(x, \eta(x)) = \sum_{j\geq 0} \frac{1}{j!}\eta^j(x)k^j\left(\frac{e^{kh}}{e^{kh}+e^{-kh}} + (-1)^j\frac{e^{-kh}}{e^{kh}+e^{-kh}}\right)e^{ikx} \tag{23}$$

which has the normalization property that $\varphi_k(x, 0) = e^{ikx}$. Relating the normal derivative of $\varphi_k(x, y)$ on the free surface,

$$\begin{aligned}
&\nabla\varphi_k(x,y)\cdot N\left(1+(\partial_x\eta(x))^2\right)^{1/2}|_{y=\eta(x)}\\
&= \sum_{j\geq 0}\frac{1}{j!}\eta^j(x)(-\partial_x\eta(x))\left(ik^{j+1}\right)\left(\frac{e^{kh}}{e^{kh}+e^{-kh}} + (-1)^j\frac{e^{-kh}}{e^{kh}+e^{-kh}}\right)e^{ikx}\\
&\quad + \sum_{j\geq 0}\frac{1}{j!}\eta^j(x)k^{j+1}\left(\frac{e^{kh}}{e^{kh}+e^{-kh}} + (-1)^{j+1}\frac{e^{-kh}}{e^{kh}+e^{-kh}}\right)e^{ikx},
\end{aligned} \tag{24}$$

to the Taylor series expansion of $G(\eta)\Phi_k$, the constant term is $G^{(0)}e^{ikx} = k\tanh(hk)e^{ikx}$. Writing this Fourier multiplication operator in terms of $D = -i\partial_x$, it reads

$$G^{(0)}e^{ikx} = D\tanh(hD)e^{ikx}. \tag{25}$$

Reading the higher terms of the Taylor expansion from (23, 24), we find

$$\begin{aligned}
G^{(j)}(\eta)e^{ikx} &= \frac{1}{j!}D\eta^j(x)D^j\left(\frac{e^{hD}}{e^{hD}+e^{-hD}} + (-1)^{j+1}\frac{e^{-hD}}{e^{hD}+e^{-hD}}\right)e^{ikx}\\
&\quad - \sum_{\ell=1}^{j} G^{(j-\ell)}(\eta)\frac{1}{\ell!}\eta^\ell(x)D^\ell\left(\frac{e^{hD}}{e^{hD}+e^{-hD}} + (-1)^\ell\frac{e^{-hD}}{e^{hD}+e^{-hD}}\right)e^{ikx},
\end{aligned} \tag{26}$$

from which one can read in a recursive manner the expressions for the Taylor coefficients of $G(\eta)$ as a function of η. In particular, one has the first- and second-order terms

$$\begin{aligned}
G^{(1)}(\eta) &= D\eta(x)D - G^{(0)}\eta(x)G^{(0)},\\
G^{(2)}(\eta) &= -\frac{1}{2}\left(D^2\eta^2(x)G^{(0)} + G^{(0)}\eta^2(x)D^2 - 2G^{(0)}\eta(x)G^{(0)}\eta(x)G^{(0)}\right),
\end{aligned} \tag{27}$$

which can also be found in (Craig and Sulem 1993). In practice in numerical computations involving the fast Fourier transform, it is more efficient in terms of computational time and memory storage to use the adjoint of the formula (26), as this only requires vector operations (Craig and Nicholls 2002).

3.2 Upper fluid domain $S_1(\eta, \eta_1)$

For the upper domain $S_1(\eta, \eta_1)$, consider the family of harmonic functions $\varphi_{1,k}(x, y) = (a(k)\, e^{ky} + b(k)\, e^{-ky})e^{ikx}$ which solve (1) with the boundary values

$$\Phi_{1,k}(x) = \Big(a(k)e^{k\eta(x)} + b(k)e^{-k\eta(x)}\Big)e^{ikx} \qquad \text{on } y = \eta(x) \tag{28}$$

$$\Phi_{2,k}(x) = \Big(a(k)e^{kh_1}e^{k\eta_1(x)} + b(k)e^{-kh_1}e^{-k\eta_1(x)}\Big)e^{ikx} \qquad \text{on } y = h_1 + \eta_1(x). \tag{29}$$

As in (23), these expressions have convergent Taylor expansions in η and in η_1 respectively;

$$\Phi_{1,k}(x) = \sum_{j\geq 0}\frac{1}{j!}\eta^j(x)k^j\big(a(k) + (-1)^j b(k)\big)e^{ikx} \tag{30}$$

$$\Phi_{2,k}(x) = \sum_{j\geq 0}\frac{1}{j!}\eta_1^j(x)k^j\big(a(k)e^{kh_1} + (-1)^j b(k)e^{-kh_1}\big)e^{ikx}. \tag{31}$$

The exterior normal derivatives of φ_1 on the two boundaries are given by

$$\begin{aligned}-\nabla\varphi_{1,k}\cdot N\Big(1 + (\partial_x\eta(x))^2\Big)^{1/2}|_{y=\eta(x)} &= \sum_{j\geq 0}\frac{1}{j!}\eta^j(x)(i\partial_x\eta(x))k^{j+1}\big(a(k) + (-1)^j b(k)\big)e^{ikx}\\ &\quad - \sum_{j\geq 0}\frac{1}{j!}\eta^j(x)k^{j+1}\Big(a(k) + (-1)^{j+1}b(k)\Big)e^{ikx}\end{aligned} \tag{32}$$

and

$$\begin{aligned}\nabla\varphi_{1,k}\cdot N_1\Big(1 + (\partial_x\eta_1(x))^2\Big)^{1/2}|_{y=h_1+\eta_1(x)} &= \sum_{j\geq 0}\frac{1}{j!}\eta_1^j(x)(-i\partial_x\eta_1(x))k^{j+1}\big(a(k)e^{h_1k}\\ + (-1)^j b(k)e^{-h_1k}\big)e^{ikx} &+ \sum_{j\geq 0}\frac{1}{j!}\eta_1^j(x)k^{j+1}\Big(a(k)e^{h_1k} + (-1)^{j+1}b(k)e^{-h_1k}\Big)e^{ikx}.\end{aligned} \tag{33}$$

Using (30, 31, 32) and (33), the relation (11) can be solved for expressions for the Taylor coefficients of the Dirichlet-Neumann operator as a double power series in η and η_1. For this, one takes a basis of the harmonic functions (28, 29), by setting in turn $(a_1(k), b_1(k)) = \big(-e^{-h_1k}/\big(e^{h_1k} - e^{-h_1k}\big), e^{h_1k}/\big(e^{h_1k} - e^{-h_1k}\big)\big), (a_2(k), b_2(k)) = \big(1/\big(e^{h_1k} - e^{-h_1k}\big), -1/\big(e^{h_1k} - e^{-h_1k}\big)\big)$. First of all, from direct comparison in the relation (11) one finds that the constant term in the Taylor expansion is

$$\begin{pmatrix} G_{11}^{(0)} & G_{12}^{(0)} \\ G_{21}^{(0)} & G_{22}^{(0)} \end{pmatrix} = \begin{pmatrix} D\coth(h_1D) & -D\,\mathrm{csch}(h_1D) \\ -D\,\mathrm{csch}(h_1D) & D\coth(h_1D) \end{pmatrix}. \tag{34}$$

We denote the general term in the Taylor expansion by $G_{j\ell}^{(m_0,m_1)}$, where $j, \ell = 1, 2$, which is homogeneous of degree m_0 in η and of degree m_1 in η_1, so that the operator can be written

$$\begin{pmatrix} G_{11}(\eta,\eta_1) & G_{12}(\eta,\eta_1) \\ G_{21}(\eta,\eta_1) & G_{22}(\eta,\eta_1) \end{pmatrix} = \sum_{m_0,m_1=0}^{\infty}\begin{pmatrix} G_{11}^{(m_0,m_1)}(\eta,\eta_1) & G_{12}^{(m_0,m_1)}(\eta,\eta_1) \\ G_{21}^{(m_0,m_1)}(\eta,\eta_1) & G_{22}^{(m_0,m_1)}(\eta,\eta_1) \end{pmatrix}.$$

The first-order terms are of particular importance in the long-wave expansions of this paper. From (30, 31, 32, 33) and the relation (11), we find

$$\begin{pmatrix} G_{11}^{(10)}(\eta,\eta_1) & G_{12}^{(10)}(\eta,\eta_1) \\ G_{21}^{(10)}(\eta,\eta_1) & G_{22}^{(10)}(\eta,\eta_1) \end{pmatrix} = \begin{pmatrix} D\coth(h_1D)\eta(x)D\coth(h_1D) - D\eta(x)D & -D\coth(h_1D)\eta(x)D\operatorname{csch}(h_1D) \\ -D\operatorname{csch}(h_1D)\eta(x)D\coth(h_1D) & D\operatorname{csch}(h_1D)\eta(x)D\operatorname{csch}(h_1D) \end{pmatrix}.$$

Similarly,

$$\begin{pmatrix} G_{11}^{(01)}(\eta,\eta_1) & G_{12}^{(01)}(\eta,\eta_1) \\ G_{21}^{(01)}(\eta,\eta_1) & G_{22}^{(01)}(\eta,\eta_1) \end{pmatrix} = \begin{pmatrix} -D\operatorname{csch}(h_1D)\eta_1(x)D\operatorname{csch}(h_1D) & D\operatorname{csch}(h_1D)\eta_1(x)D\coth(h_1D) \\ D\coth(h_1D)\eta_1(x)D\operatorname{csch}(h_1D) & -D\coth(h_1D)\eta_1(x)D\coth(h_1D) + D\eta_1(x)D \end{pmatrix}.$$

There is a recursion formula for the higher-order terms in the Taylor series expansion for $G_{j\ell}^{(m)}(\eta,\eta_1)$, analogous to the concise formula (26) whose details are given in the Appendix.

4 Linear analysis

We begin our analysis by examining the linearized equations about the fluid at rest. This amounts to truncating the Taylor expansion of the Hamiltonian at its quadratic terms.

4.1 Linearized equations

Using (9) and (21), as well as the lowest-order terms in the expressions of the Dirichlet-Neumann operators, the quadratic part of the Hamiltonian is given by

$$H^{(2)} = \frac{1}{2}\int_{\mathbb{R}} \xi \frac{D\tanh(hD)\coth(h_1D)}{\rho\coth(h_1D)+\rho_1\tanh(hD)}\xi + 2\xi\frac{D\tanh(hD)\operatorname{csch}(h_1D)}{\rho\coth(h_1D)+\rho_1\tanh(hD)}\xi_1 + \xi_1\frac{D(\coth(h_1D)\tanh(hD)+\rho/\rho_1)}{\rho\coth(h_1D)+\rho_1\tanh(hD)}\xi_1 + g(\rho-\rho_1)\eta^2 + g\rho_1\eta_1^2 dx. \tag{35}$$

The linearized equations of motion are

$$\begin{aligned} \partial_t\eta &= \delta_\xi H^{(2)} = \frac{D\tanh(hD)\coth(h_1D)}{\rho\coth(h_1D)+\rho_1\tanh(hD)}\xi + \frac{D\tanh(hD)\operatorname{csch}(h_1D)}{\rho\coth(h_1D)+\rho_1\tanh(hD)}\xi_1 \\ \partial_t\xi &= -\delta_\eta H^{(2)} = -g(\rho-\rho_1)\eta, \end{aligned}$$

and

$$\begin{aligned} \partial_t\eta_1 &= \delta_{\xi_1} H^{(2)} = \frac{D\tanh(hD)\operatorname{csch}(h_1D)}{\rho\coth(h_1D)+\rho_1\tanh(hD)}\xi \\ &\quad + \frac{D(\coth(h_1D)\tanh(hD)+\rho/\rho_1)}{\rho\coth(h_1D)+\rho_1\tanh(hD)}\xi_1 \\ \partial_t\xi_1 &= -\delta_{\eta_1} H^{(2)} = -g\rho_1\eta_1. \end{aligned} \tag{36}$$

The corresponding dispersion relation for ω^2 is determined by the quadratic equation

$$\omega^4 - g\rho k \frac{1+\tanh(kh)\coth(kh_1)}{\rho\coth(kh_1)+\rho_1\tanh(kh)}\omega^2 + g^2(\rho-\rho_1)k^2\frac{\tanh(kh)}{\rho\coth(kh_1)+\rho_1\tanh(kh)} = 0. \tag{37}$$

The two solutions $\omega^{\pm}(k)$ of (37) are associated with two different modes of wave motion, namely surface and interface displacements. These represent the temporal frequencies of the two modes in the normal mode decomposition of the Hamiltonian system for each wave number k. They are given by

$$\begin{aligned}\left(\omega^{\pm}\right)^2 = &\frac{1}{2}g\rho k\frac{1+\tanh(hk)\coth(\mathrm{h_1k})}{\rho\coth(h_1k)+\rho_1\tanh(hk)}\\ &\pm\frac{1}{2}gk\Big[\rho^2(1-\tanh(hk)\coth(h_1k))^2\\ &+4\rho\rho_1\tanh(hk)(\coth(h_1k)-\tanh(hk))\\ &+4\rho_1^2\tanh(hk)^2\Big]^{1/2}/(\rho\coth(h_1k)+\rho_1\tanh(hk)).\end{aligned} \tag{38}$$

The radicand is always positive, as can be assured by the fact that for all wavenumbers $k>0, \tanh(hk)<1<\coth(h_1k)$. The branch $\omega^+(k) := \omega_1(k)$ is associated with free surface wave motion, while the linear behavior of the interface mode is governed by $\omega^-(k) := \omega(k)$.

4.2 Comparison with the rigid lid case

It is important to compare the dispersion relation ω^- for the interfacial mode with the dispersion relation ω for the case of a rigid lid, as given by

$$\omega^2 = \frac{g(\rho-\rho_1)k\tanh(kh)\tanh(kh_1)}{\rho\tanh(kh_1)+\rho_1\tanh(kh)}.$$

In the regime where $k\to+\infty$, fixing other aspects of the fluid domain, one finds

$$\left(\omega_\infty^+\right)^2 = gk, \quad \left(\omega_\infty^-\right)^2 = \frac{g(\rho-\rho_1)}{\rho+\rho_1}k. \tag{39}$$

The latter agrees with the asymptotics as $k\to+\infty$ of the dispersion relation for the rigid lid case. The expression $\left(\omega_\infty^+\right)^2 = gk$ agrees with the dynamics of the free surface with no interface present.

However, the behavior of the dispersion relations for long-wave regimes are very different when considering the case of a free surface lying over a free interface and the case of rigid lid upper boundary conditions. Letting kh and $kh_1\to 0$ while fixing the ratio h/h_1 to be finite, one finds that the two phase speeds associated with the two branches of the dispersion curve $\omega^{\pm}$ are asymptotic to

$$\left(c_0^{\pm}\right)^2 = \frac{1}{2}g\left(h+h_1\pm\sqrt{(h-h_1)^2+4\frac{\rho_1}{\rho}hh_1}\right). \tag{40}$$

We only consider $\rho_1<\rho$, so the 'faster' free surface phase velocity c_0^+ is somewhat slower than if there were no interface present. Note that the phase velocity $\left(c_0^-\right)^2$ associated with the free interface (the 'slower' dispersion curve) is positive for $\rho>\rho_1$ (stable

stratification). Examining c_0^-, we conclude that it can behave completely differently than the case of the rigid lid, as given by

$$c_0^2 = \frac{g(\rho - \rho_1)}{\rho/h + \rho_1/h_1}.$$

There is also a significant difference between the dispersive behavior in this long-wave regime, in the case of a free surface and a free interface, compared to the case of a rigid lid.

In other situations, such as when $kh \to \infty$ (infinitely deep lower layer) and $kh_1 \to 0$ (finite upper layer),

$$\left(c_0^+\right)^2 = \frac{g}{k} \quad \text{and} \quad \left(c_0^-\right)^2 = gh_1\left(1 - \frac{\rho_1}{\rho}\right). \tag{41}$$

This differs from the regime of two finite layers where both $\left(c_0^\pm\right)^2$ are of the same order of magnitude, as shown in (40).

In Fig. 2, we plot the linear phase speeds for the different configurations as functions of the wavenumber. The linear phase speed $c = \omega/k$ for the interface in the rigid lid case is given by

$$c = \sqrt{\frac{g(\rho - \rho_1)\tanh(kh)\tanh(kh_1)}{k(\rho\tanh(kh_1) + \rho_1\tanh(kh))}},$$

while those of the coupled system are given by (38) ($c^\pm = \omega^\pm/k$). We show the comparison between c and $c^\pm$ for two different values of the density ratio $\rho_1/\rho = 0.1, 0.9$ and for three different values of the depth ratio $h_1/h = 10, 1, 0.1$. As expected, c^- coincides with c at large k and their graphs always lie below that of c^+. The differences between c and c^- are most significant for small values of ρ_1/ρ. Also the values of c and c^- are slightly larger for small ρ_1/ρ than for large ρ_1/ρ. This is the fact that interfacial waves propagate more rapidly beneath a less dense fluid. For a given value of ρ_1/ρ, the differences between c and c^- are most important when the ratio h_1/h is small. When h_1/h is large, their graphs match perfectly since in this case the effects of a rigid lid or a free surface are negligible.

5 Coupled KdV-modulational regime

5.1 Normal mode decomposition

We focus on the situation of two finite fluid layers and where both the interface and surface are of small amplitude. Since we are dealing with a coupled system, it is convenient to perform a normal mode decomposition in order to simplify the quadratic part of the Hamiltonian. This is effected by applying the canonical transformations

$$\begin{pmatrix} \eta' \\ \xi' \\ \eta_1' \\ \xi_1' \end{pmatrix} = \begin{pmatrix} \sqrt{g(\rho-\rho_1)} & 0 & 0 & 0 \\ 0 & \frac{1}{\sqrt{g(\rho-\rho_1)}} & 0 & 0 \\ 0 & 0 & \sqrt{g\rho_1} & 0 \\ 0 & 0 & 0 & \frac{1}{\sqrt{g\rho_1}} \end{pmatrix} \begin{pmatrix} \eta \\ \xi \\ \eta_1 \\ \xi_1 \end{pmatrix}, \tag{42}$$

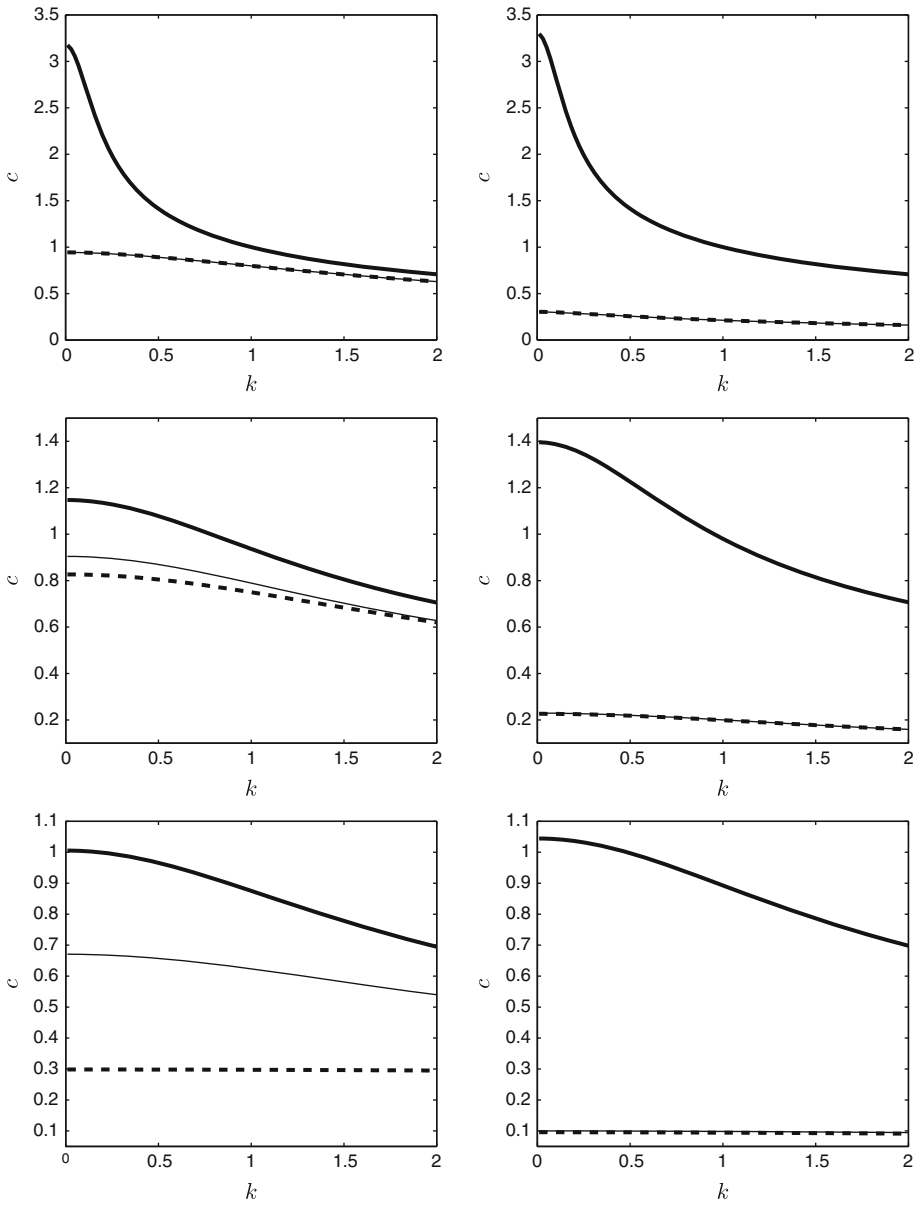

Fig. 2 Linear phase speed c vs. wavenumber k for $\rho_1/\rho = 0.1$ (*left*) and $\rho_1/\rho = 0.9$ (*right*): $h_1/h = 10$ (*top*), $h_1/h = 1$ (*middle*), $h_1/h = 0.1$ (*bottom*). The linear phase speed c for the interface in the rigid lid case is represented in *thin solid line*. The linear phase speeds c^- and c^+ in the coupled system are represented in thick *dashed* and *solid lines*, respectively

and

$$\begin{pmatrix} \mu \\ \zeta \\ \mu_1 \\ \zeta_1 \end{pmatrix} = \begin{pmatrix} a^- & 0 & b^- & 0 \\ 0 & a^- & 0 & b^- \\ a^+ & 0 & b^+ & 0 \\ 0 & a^+ & 0 & b^+ \end{pmatrix} \begin{pmatrix} \eta' \\ \xi' \\ \eta'_1 \\ \xi'_1 \end{pmatrix}, \tag{43}$$

where

$$\begin{aligned} a^{\pm}(D) &= \left(2 + \frac{\theta^2}{2} \pm \frac{\theta}{2}\sqrt{4+\theta^2}\right)^{-1/2}, \quad \theta = \frac{C(D) - A(D)}{B(D)}, \\ b^{\pm}(D) &= \frac{1}{2}\left(\theta \pm \sqrt{4+\theta^2}\right)\left(2 + \frac{\theta^2}{2} \pm \frac{\theta}{2}\sqrt{4+\theta^2}\right)^{-1/2}, \end{aligned} \tag{44}$$

and the coefficients $A(D)$, $B(D)$ and $C(D)$ are the coefficients appearing in the expression (35) of $H^{(2)}$ and defined by

$$\begin{aligned} A(D) &= \frac{g(\rho - \rho_1)D\tanh(hD)\coth(h_1 D)}{\rho\coth(h_1 D) + \rho_1\tanh(hD)}, \\ B(D) &= \frac{g\sqrt{\rho_1(\rho-\rho_1)}D\tanh(hD)\operatorname{csch}(h_1 D)}{\rho\coth(h_1 D) + \rho_1\tanh(hD)}, \\ C(D) &= \frac{g\rho_1 D(\coth(h_1 D)\tanh(hD) + \rho/\rho_1)}{\rho\coth(h_1 D) + \rho_1\tanh(hD)}. \end{aligned}$$

As a result, the quadratic part of the Hamiltonian takes the simpler form

$$H^{(2)} = \frac{1}{2}\int_{\mathbb{R}} \zeta\omega^2(D)\zeta + \mu^2 + \zeta_1\omega_1^2(D)\zeta_1 + \mu_1^2 dx, \tag{45}$$

where

$$\begin{aligned} \omega^2(D) &= \frac{1}{2}\left(A(D) + C(D) - \sqrt{(A(D)-C(D))^2 + 4B^2(D)}\right), \\ \omega_1^2(D) &= \frac{1}{2}\left(A(D) + C(D) + \sqrt{(A(D)-C(D))^2 + 4B^2(D)}\right) \end{aligned}$$

are the eigenvalues of the symmetric matrix $\begin{pmatrix} A & B \\ B & C \end{pmatrix}$, which coincide with the two roots $(\omega^{\pm})^2$ of the quadratic Eq. 37 defining the dispersion relation. Of course the operators $A(D)$, $B(D)$, $C(D)$, $\theta(D)$, etc. are differential operators, but as they mutually commute the calculation makes sense, and in the case of $B^{-1}(D)$ the possible singularity of $\theta(D)$ at zero is regularized due to cancellations in $C(D) - A(D)$. Through this transformation, the equations of motion (22) are transformed to

$$\partial_t \begin{pmatrix} \mu \\ \zeta \\ \mu_1 \\ \zeta_1 \end{pmatrix} = \begin{pmatrix} 0 & 1 & 0 & 0 \\ -1 & 0 & 0 & 0 \\ 0 & 0 & 0 & 1 \\ 0 & 0 & -1 & 0 \end{pmatrix} \begin{pmatrix} \delta_\mu H \\ \delta_\zeta H \\ \delta_{\mu_1} H \\ \delta_{\zeta_1} H \end{pmatrix}.$$

Of course the higher-order terms of the Hamiltonian are transformed as well by these changes of variables.

Since both internal and surface waves propagate with their respective speeds, it is also convenient to change the equations to a moving reference frame. In the present Hamiltonian setting, this is accommodated by subtracting a multiple of the momentum (i.e., the impulse integral)

$$I = \int_{\mathbb{R}} \left(\rho \int_{-h}^{\eta(x)} \partial_x \varphi dy + \rho_1 \int_{\eta(x)}^{h_1+\eta_1(x)} \partial_x \varphi_1 dy \right) dx$$
$$= -\int_{\mathbb{R}} (\xi \partial_x \eta + \xi_1 \partial_x \eta_1) dx = -\int_{\mathbb{R}} (\zeta \partial_x \mu + \zeta_1 \partial_x \mu_1) dx, \tag{46}$$

from the Hamiltonian, $H \to H - cI$. It is possible to do so because the total momentum (46) is also a conserved quantity of the coupled system.

5.2 Long-wave scaling and the modulational Ansatz

Next, we introduce the scaling regime we are interested to describe. We assume that the 'internal' modes are long waves according to the scalings

$$X = \varepsilon x, \quad \mu(x,t) = \varepsilon^2 \tilde{\mu}(X,t), \quad \zeta(x,t) = \varepsilon \tilde{\zeta}(X,t),$$

where $\varepsilon^2 = (h/\lambda)^2 = a/h \ll 1$ (with a and λ being the typical internal wave amplitude and wavelength respectively), and the 'surface' modes are quasi-monochromatic waves obeying the modulational Ansatz, which after an additional canonical transformation takes the form

$$\mu_1(x,t) = \frac{\varepsilon_1}{\sqrt{2}} \omega_1^{1/2}(D)\left(v_1(X,t)e^{ik_0 x} + \bar{v}_1(X,t)e^{-ik_0 x}\right) + \varepsilon_1^2 \tilde{\mu}_1(X,t), \quad \tilde{\mu}_1 = P_0 \mu_1,$$
$$\zeta_1(x,t) = \frac{\varepsilon_1}{\sqrt{2}i} \omega_1^{-1/2}(D)\left(v_1(X,t)e^{ik_0 x} - \bar{v}_1(X,t)e^{-ik_0 x}\right) + \frac{\varepsilon_1^2}{\varepsilon} \tilde{\zeta}_1(X,t), \quad \tilde{\zeta}_1 = P_0 \zeta_1,$$

where $\varepsilon_1 = k_0 a_1 \ll 1$ (with a_1 and k_0 being the typical surface wave amplitude and carrier wavenumber, respectively). A more precise relationship between ε and ε_1 will be fixed below. We note that several regimes in the modulation theory of free surface waves and internal waves have been described in (Hashizume 1980), precisely by imposing relations between ε and ε_1. The symbol $\bar{}$ denotes complex conjugation, and P_0 is the projection that associates to μ_1 and ξ_1 their zero-frequency components. Therefore, v_1 represents the envelope of the surface modes, and $\tilde{\mu}_1$ and $\tilde{\xi}_1$ the associated mean flows (Craig et al. 2010).

The next step is to substitute these scalings and Ansatz in the Hamiltonian and perform expansions. This approach combines calculations of (Craig and Groves 1994; Craig et al. 2005a, 2010) devoted to the derivations of KdV and NLS-like equations in a Hamiltonian setting. The leading term in the Hamiltonian is naturally $H^{(2)}$ as given by (45). In (45), $\omega(D)$, acting on functions of $X = \varepsilon x$ is replaced by $\omega(\varepsilon D_X)$ while $\omega_1(D)$ acting on functions of x and X is replaced by $\omega_1(D_x + \varepsilon D_X)$. To get the Boussinesq-KdV like terms, we need in addition to compute the next-order corrections to the quadratic Hamiltonian. The resulting Hamiltonian expansion is then obtained in the form

$$
\begin{aligned}
H = \int_{\mathbb{R}} \Bigg[& \frac{1}{2}\varepsilon\tilde{\zeta}\Big(\omega^2(0) + \varepsilon\omega^2(0)' D_X + \frac{1}{2}\varepsilon^2\omega^2(0)'' D_X^2 + \frac{1}{6}\varepsilon^3\omega^2(0)''' D_X^3 \\
& + \frac{1}{24}\varepsilon^4\omega^2(0)'''' D_X^4\Big)\tilde{\zeta} + \frac{1}{2}\varepsilon^3\tilde{\mu}^2 + \frac{1}{2}\varepsilon^5\kappa\tilde{\mu}(D_X\tilde{\zeta})^2 \\
& + \frac{\varepsilon_1^2}{\varepsilon}\bar{v}_1\Big(\omega_1(k_0) + \varepsilon\omega_1'(k_0)D_X + \frac{1}{2}\varepsilon^2\omega_1''(k_0)D_X^2\Big)v_1 \\
& + \frac{1}{2}\frac{\varepsilon_1^4}{\varepsilon^3}\tilde{\zeta}_1\Big(\omega_1^2(0) + \varepsilon\omega_1^2(0)' D_X + \frac{1}{2}\varepsilon^2\omega_1^2(0)'' D_X^2\Big)\tilde{\zeta}_1 + \frac{1}{2}\frac{\varepsilon_1^4}{\varepsilon}\tilde{\mu}_1^2 \\
& + \varepsilon\varepsilon_1^2\Big(\kappa_1\tilde{\mu} + i\kappa_2 D_X\tilde{\zeta}\Big)|v_1|^2 + \frac{\varepsilon_1^4}{\varepsilon}\Big(\kappa_3\tilde{\mu}_1 + i\kappa_4 D_X\tilde{\zeta}_1\Big)|v_1|^2 \\
& + \frac{\varepsilon_1^4}{\varepsilon}\kappa_5|v_1|^4 + \cdots\Bigg] dX,
\end{aligned}
$$

where the coefficients $\omega^2(0), \omega^2(0)', \omega^2(0)''', \omega_1^2(0)$ and $\omega_1^2(0)'$ can be shown to be zero,

$$
\begin{aligned}
\kappa = & -\frac{\sqrt{g(\rho-\rho_1)}}{\rho}a^-(0)^3 - 2\frac{\sqrt{g\rho_1}}{\rho}a^-(0)^2 b^-(0) \\
& - \sqrt{\frac{g}{\rho_1}}b^-(0)^3 + \frac{\sqrt{g(\rho-\rho_1)}}{\rho}a^-(0)b^-(0)^2,
\end{aligned} \tag{47}
$$

and the other coefficients κ_i have explicit expressions as well. The notation f' stands for differentiation with respect to the argument of f. Similarly,

$$
I = -\int_{\mathbb{R}}\Big[i\varepsilon^3\tilde{\zeta}D_X\tilde{\mu} - \frac{\varepsilon_1^2}{\varepsilon}k_0|v_1|^2 - \frac{1}{2}\varepsilon_1^2\big(\bar{v}_1 D_X v_1 + v_1\overline{D_X v_1}\big) - i\frac{\varepsilon_1^4}{\varepsilon}\tilde{\mu}_1 D_X\tilde{\zeta}_1 + \cdots\Big]dX.
$$

Combining these two quantities, we obtain

$$
\begin{aligned}
H - cI = \int_{\mathbb{R}} \Bigg[& \frac{\varepsilon_1^2}{\varepsilon}(\omega_1(k_0) - ck_0)|v_1|^2 + \frac{1}{2}\varepsilon_1^2\big(\omega_1'(k_0) - c\big)\big(\bar{v}_1 D_X v_1 + v_1\overline{D_X v_1}\big) \\
& + \frac{1}{4}\varepsilon^3\omega^2(0)''\left[\frac{2\tilde{\mu}^2}{\omega^2(0)''}\left(1 - \frac{2c^2}{\omega^2(0)''}\right) - \left(D_X\tilde{\zeta} + \frac{2ic\tilde{\mu}}{\omega^2(0)''}\right)^2\right] \\
& + \varepsilon^5\left[\frac{1}{48}\omega^2(0)''''\left(D_X^2\tilde{\zeta}\right)^2 + \frac{1}{2}\kappa\tilde{\mu}(D_X\tilde{\zeta})^2\right] \\
& + \frac{1}{2}\varepsilon\varepsilon_1^2\omega_1''(k_0)\bar{v}_1 D_X^2 v_1 - \frac{1}{4}\frac{\varepsilon_1^4}{\varepsilon}\omega_1^2(0)''(D_X\tilde{\zeta}_1)^2 + \frac{1}{2}\frac{\varepsilon_1^4}{\varepsilon}\tilde{\mu}_1^2 \\
& + \varepsilon\varepsilon_1^2\Big(\kappa_1\tilde{\mu} + i\kappa_2 D_X\tilde{\zeta}\Big)|v_1|^2 + \frac{\varepsilon_1^4}{\varepsilon}\Big(\kappa_3\tilde{\mu}_1 + i\kappa_4 D_X\tilde{\zeta}_1\Big)|v_1|^2 \\
& + \frac{\varepsilon_1^4}{\varepsilon}\kappa_5|v_1|^4 - ic\frac{\varepsilon_1^4}{\varepsilon}\tilde{\mu}_1 D_X\tilde{\zeta}_1 + \cdots\Bigg] dX.
\end{aligned} \tag{48}
$$

The change of variables $(\mu, \zeta, \mu_1, \zeta_1) \to \left(\tilde{\mu}, \tilde{\zeta}, v_1, \bar{v}_1, \tilde{\mu}_1, \tilde{\zeta}_1\right)$, together with the spatial scaling $x \to X = \varepsilon x$, leads to a change in the symplectic matrix. Namely, J as defined in (22) is replaced by

$$J_1 = \begin{pmatrix} 0 & \varepsilon^{-2} & 0 & 0 & 0 & 0 \\ -\varepsilon^{-2} & 0 & 0 & 0 & 0 & 0 \\ 0 & 0 & 0 & -i\varepsilon\varepsilon_1^{-2}\mathbb{I}' & 0 & 0 \\ 0 & 0 & i\varepsilon\varepsilon_1^{-2}\mathbb{I}' & 0 & 0 & 0 \\ 0 & 0 & 0 & 0 & 0 & \varepsilon^2\varepsilon_1^{-4} \\ 0 & 0 & 0 & 0 & -\varepsilon^2\varepsilon_1^{-4} & 0 \end{pmatrix}, \tag{49}$$

where $\mathbb{I}'$ is the identity operator on the class of functions of X, and the two opposite 2×2 blocks essentially retain the standard symplectic form on the spaces of functions $\left(\tilde{\mu}, \tilde{\zeta}\right)$ and $\left(\tilde{\mu}_1, \tilde{\zeta}_1\right)$. The corresponding equations of motion read

$$\partial_t U = J_1 \nabla_U (H - cI), \tag{50}$$

where $U = \left(\tilde{\mu}, \tilde{\zeta}, v_1, \bar{v}_1, \tilde{\mu}_1, \tilde{\zeta}_1\right)^\top$.

5.3 Resonance condition

Equation 48 indicates that $H - c\,I$ can be further simplified by choosing c such that

$$c = c_0 = \sqrt{\frac{\omega^2(0)''}{2}} = \sqrt{\frac{g}{2}}\left(h + h_1 - \sqrt{(h-h_1)^2 + 4\frac{\rho_1}{\rho}hh_1}\right)^{1/2}, \tag{51}$$

and moreover, if k_0 is selected such that

$$\omega_1'(k_0) = c_0, \tag{52}$$

then (48) reduces to

$$\begin{aligned} H - c_0 I = \int_{\mathbb{R}} & \frac{\varepsilon_1^2}{\varepsilon}(\omega_1(k_0) - c_0 k_0)|v_1|^2 - \frac{1}{2}\varepsilon^3\left(c_0 D_X\tilde{\zeta} + i\tilde{\mu}\right)^2 \\ & + \varepsilon^5\left[\frac{1}{48}\omega^2(0)''''\left(D_X^2\tilde{\zeta}\right)^2 + \frac{1}{2}\kappa\tilde{\mu}\left(D_X\tilde{\zeta}\right)^2\right] \\ & + \frac{1}{2}\varepsilon\varepsilon_1^2\omega_1''(k_0)\bar{v}_1 D_X^2 v_1 - \frac{1}{4}\frac{\varepsilon_1^4}{\varepsilon}\omega_1^2(0)''\left(D_X\tilde{\zeta}_1\right)^2 + \frac{1}{2}\frac{\varepsilon_1^4}{\varepsilon}\tilde{\mu}_1^2 \\ & + \varepsilon\varepsilon_1^2\left(\kappa_1\tilde{\mu} + i\kappa_2 D_X\tilde{\zeta}\right)|v_1|^2 + \frac{\varepsilon_1^4}{\varepsilon}\left(\kappa_3\tilde{\mu}_1 + i\kappa_4 D_X\tilde{\zeta}_1\right)|v_1|^2 \\ & + \frac{\varepsilon_1^4}{\varepsilon}\kappa_5|v_1|^4 - ic_0\frac{\varepsilon_1^4}{\varepsilon}\tilde{\mu}_1 D_X\tilde{\zeta}_1 + \cdots\Big]dX. \end{aligned} \tag{53}$$

Note that c is determined by ω according to (51), while (52) involves ω_1. Therefore, Eq. 52 can be thought of as a linear resonance condition between the internal and surface modes.

Figures 3 and 4 plot numerical solutions k_0 of (52) for different values of the density ratio ρ_1/ρ and depth ratio h_1/h. The left hand side $\omega_1'(k_0)$ of (52) has a rather complicated expression and is not shown here for convenience. Note that $\rho_1/\rho = 0.99$ is a typical value in realistic conditions. The main observation is that there is always a surface mode of wavenumber k_0 which satisfies the resonance condition (52), and thus travels at the same linear speed as a long internal mode. The smaller h_1/h, or the closer ρ_1/ρ to unity, the larger k_0 (and hence the shorter the surface mode). In addition, although k_0 varies monotonically as a function of h_1/h and ρ_1/ρ, we clearly distinguish in all cases two regions where k_0 varies very rapidly and then much more slowly in the limits $h_1/h \to 0$ and $\rho_1/\rho \to 1$.

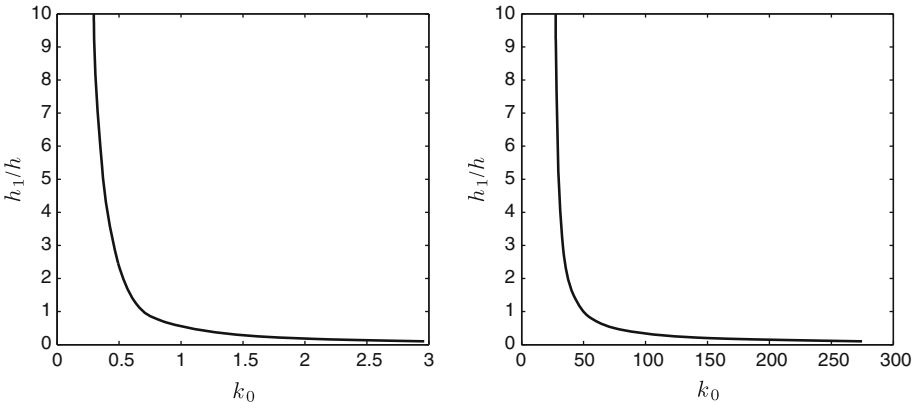

Fig. 3 Depth ratio h_1/h vs. wavenumber k_0 corresponding to the linear resonance condition for $\rho_1/\rho = 0.1$ (*left*) and $\rho_1/\rho = 0.99$ (*right*)

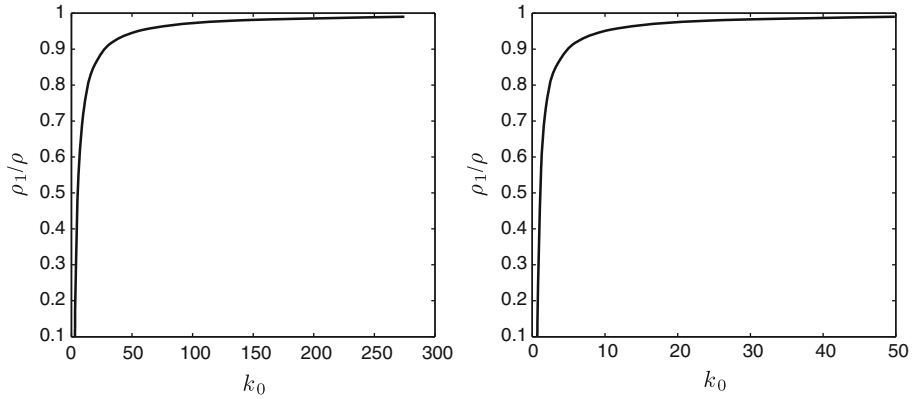

Fig. 4 Density ratio ρ_1/ρ vs. wavenumber k_0 corresponding to the linear resonance condition for $h_1/h = 0.1$ (*left*) and $h_1/h = 1$ (*right*)

Now assuming $\varepsilon_1 = \varepsilon^{2+\alpha}$ (with $0 < \alpha \leq 1/2$), which is to say that the surface modes are of smaller amplitude than the internal modes, and retaining terms of order $O(\varepsilon^5)$ only, we obtain

$$H - c_0 I = \int_{\mathbb{R}} \varepsilon^{3+2\alpha}(\omega_1(k_0) - c_0 k_0)|v_1|^2 - \frac{1}{2}\varepsilon^3\left(c_0 D_X\tilde{\zeta} + i\tilde{\mu}\right)^2 + \varepsilon^5\left[\frac{1}{48}\omega^2(0)''''\left(D_X^2\tilde{\zeta}\right)^2 + \frac{1}{2}\kappa\tilde{\mu}\left(D_X\tilde{\zeta}\right)^2\right]dX + O\left(\varepsilon^5\right).$$

At this order of approximation, we note that the L^2 norm

$$M = \int_{\mathbb{R}} |v_1|^2 dX,$$

is also a conserved quantity of the system, which can be easily verified by showing that M Poisson commutes with $H - c\ I$. This property is related to the phase invariance of the approximate solutions and can be accommodated by subtracting a multiple of M from $H - c\ I$. Therefore, at the order of approximation considered, the renormalized Hamiltonian

$$\begin{aligned}\hat{H} &= H - c_0 I - \varepsilon^{3+2\alpha}(\omega_1(k_0) - c_0 k_0)M \\ &= -\int_{\mathbb{R}} \frac{1}{2}\varepsilon^3 \left(c_0 D_X \tilde{\zeta} + i\tilde{\mu}\right)^2 \\ &\quad - \varepsilon^5 \left[\frac{1}{48}\omega^2(0)'''' \left(D_X^2 \tilde{\zeta}\right)^2 + \frac{1}{2}\kappa\tilde{\mu}(D_X\tilde{\zeta})^2\right] dX,\end{aligned}$$

describes the essential dynamics of the system. If we make the further change of variables $\tilde{u} = \partial_X \tilde{\zeta}$ (which plays the role of a horizontal shear velocity), then

$$\hat{H} = \int_{\mathbb{R}} \frac{1}{2}\varepsilon^3(\tilde{\mu} - c_0\tilde{u})^2 + \varepsilon^5 \left[\frac{1}{48}\omega^2(0)''''(\partial_X \tilde{u})^2 - \frac{1}{2}\kappa\tilde{\mu}\tilde{u}^2\right] dX, \tag{54}$$

and the equations of motion are transformed to

$$\partial_t \begin{pmatrix} \tilde{\mu} \\ \tilde{u} \\ \nu_1 \\ \bar{\nu}_1 \\ \tilde{\mu}_1 \\ \tilde{\zeta}_1 \end{pmatrix} = \begin{pmatrix} 0 & -\varepsilon^{-2}\partial_X & 0 & 0 & 0 & 0 \\ -\varepsilon^{-2}\partial_X & 0 & 0 & 0 & 0 & 0 \\ 0 & 0 & 0 & -i\varepsilon^{-3-2\alpha}\mathbb{I}' & 0 & 0 \\ 0 & 0 & i\varepsilon^{-3-2\alpha}\mathbb{I}' & 0 & 0 & 0 \\ 0 & 0 & 0 & 0 & 0 & \varepsilon^{-6-4\alpha} \\ 0 & 0 & 0 & 0 & -\varepsilon^{-6-4\alpha} & 0 \end{pmatrix} \begin{pmatrix} \delta_{\tilde{\mu}}\hat{H} \\ \delta_{\tilde{u}}\hat{H} \\ \delta_{\nu_1}\hat{H} \\ \delta_{\bar{\nu}_1}\hat{H} \\ \delta_{\tilde{\mu}_1}\hat{H} \\ \delta_{\tilde{\zeta}_1}\hat{H} \end{pmatrix}.$$

This indicates that the internal and surface wave motions are decoupled at order $O(\varepsilon^5)$, with the internal modes obeying the Boussinesq equations

$$\begin{aligned}\partial_t \tilde{\mu} &= -\partial_X \left[c_0(c_0\tilde{u} - \tilde{\mu}) - \varepsilon^2 \left(\frac{1}{24}\omega^2(0)''''\partial_X^2\tilde{u} + \kappa\tilde{\mu}\tilde{u}\right)\right], \\ \partial_t \tilde{u} &= -\partial_X \left(\tilde{\mu} - c_0\tilde{u} - \frac{1}{2}\varepsilon^2\kappa\tilde{u}^2\right),\end{aligned}$$

after rescaling $t \to \varepsilon t$.

5.4 A KdV equation for the interface

The next step is to look at the dynamics of the system in a preferred direction of propagation. This is achieved by adopting the characteristic variables

$$\begin{pmatrix} r \\ s \end{pmatrix} = \begin{pmatrix} \frac{1}{\sqrt{2c_0}} & \sqrt{\frac{c_0}{2}} \\ \frac{1}{\sqrt{2c_0}} & -\sqrt{\frac{c_0}{2}} \end{pmatrix} \begin{pmatrix} \tilde{\mu} \\ \tilde{u} \end{pmatrix},$$

where $r(X, t)$ is the component of the solution that is principally right-moving, while $s(X, t)$ is principally left-moving. In terms of these variables, Eq. 54 reads

$$\hat{H} = \int_{\mathbb{R}} \varepsilon^3 c_0 s^2 + \varepsilon^5 \frac{\omega^2(0)''''}{96c_0}\left[(\partial_X r)^2 - 2(\partial_X r)(\partial_X s) + (\partial_X s)^2\right] - \varepsilon^5\sqrt{\frac{c_0}{2}}\frac{\kappa}{4c_0}\left(r^3 - r^2 s - r s^2 + s^3\right)dX,$$

and the corresponding equations of motion are

$$\partial_t \begin{pmatrix} r \\ s \\ v_1 \\ \bar{v}_1 \\ \tilde{\mu}_1 \\ \tilde{\zeta}_1 \end{pmatrix} = \begin{pmatrix} -\varepsilon^{-2}\partial_X & 0 & 0 & 0 & 0 & 0 \\ 0 & \varepsilon^{-2}\partial_X & 0 & 0 & 0 & 0 \\ 0 & 0 & 0 & -i\varepsilon^{-3-2\alpha}\mathbb{I}' & 0 & 0 \\ 0 & 0 & i\varepsilon^{-3-2\alpha}\mathbb{I}' & 0 & 0 & 0 \\ 0 & 0 & 0 & 0 & 0 & \varepsilon^{-6-4\alpha} \\ 0 & 0 & 0 & 0 & -\varepsilon^{-6-4\alpha} & 0 \end{pmatrix} \begin{pmatrix} \delta_r \hat{H} \\ \delta_s \hat{H} \\ \delta_{v_1} \hat{H} \\ \delta_{\bar{v}_1} \hat{H} \\ \delta_{\tilde{\mu}_1} \hat{H} \\ \delta_{\tilde{\zeta}_1} \hat{H} \end{pmatrix}. \tag{55}$$

The KdV regime consists of restricting one's attention to the region of phase space where s is of order $O(\varepsilon^2)$, which is to say that one focuses primarily on the propagation to the right. In this situation, retaining only terms of order $O(\varepsilon^5)$ leads to

$$\hat{H} = \int_{\mathbb{R}} \varepsilon^5 \frac{\omega^2(0)''''}{96c_0}(\partial_X r)^2 - \varepsilon^5\sqrt{\frac{c_0}{2}}\frac{\kappa}{4c_0} r^3 dX,$$

and the evolution equation for r, $\partial_t r = -\varepsilon^{-2}\partial_X \delta_r \hat{H}$, can be rewritten as

$$\partial_\tau r = \frac{\omega^2(0)''''}{48c_0}\partial_X^3 r + \sqrt{\frac{c_0}{2}}\frac{3\kappa}{2c_0} r\partial_X r, \tag{56}$$

which is a KdV equation expressed in a reference frame moving at speed c_0 and evolving over time scale $\tau = \varepsilon^3 t$.

5.5 A linear Schrödinger equation for the free surface

If the higher-order terms in (53) are taken into account, the evolution equations for the surface modes $v_1, \tilde{\mu}_1$ and $\tilde{\zeta}_1$ can be obtained from (55). The equation for v_1 reads

$$\partial_{\tau_1} v_1 = i\left[\frac{1}{2}\omega_1''(k_0)\partial_X^2 v_1 + \tilde{\kappa}_1 r v_1 + \varepsilon^{2+2\alpha}\left(\tilde{\kappa}_3\tilde{\mu}_1 + \tilde{\kappa}_4\partial_X\tilde{\zeta}_1 + \tilde{\kappa}_5|v_1|^2\right)v_1\right], \tag{57}$$

where $\tau_1 = \varepsilon^2 t$ is the usual scaling time in modulational analysis. We note that the nonlinear term appears at a much higher order. Thus, at leading order, v_1 satisfies a linear Schrödinger equation with an external potential proportional to the solution r of the KdV equation describing the internal modes,

$$-i\partial_{\tau_1} v_1 = \frac{1}{2}\omega_1''(k_0)\partial_X^2 v_1 + \tilde{\kappa}_1 r v_1. \tag{58}$$

In general, the Schrödinger operator on the right-hand side of this equation has a time-dependent potential, and there are few general statements that one can make about its solutions. However, in the important case of an internal wave soliton, the Schrödinger operator appearing in (58) can be reduced to a time-independent potential. In particular, when $\tilde{\kappa}_1 r > 0$, the potential has eigenvalues whose associated eigenfunctions are localized bound states in

the reference frame of the soliton. In this situation, the wave pattern exhibited by this trapped free surface mode is visible in the vicinity of the soliton peak, and travels with it. We propose that these trapped modes are the cause of the changes in surface reflectancy that so very dramatically affect the imaging of internal waves. Thus the trapped modes can be considered as an effective signature for the presence of this type of internal waves.

When rigid lid boundary conditions are imposed and $r(X, t)$ represents a soliton internal wave, then the sign of the profile of r is determined by the sign of

$$\rho h_1^2 - \rho_1 h^2, \tag{59}$$

as given in (Benjamin 1966). In the free interface-free surface problem, the relative sign of the dispersive and nonlinear terms of (56) are what determines this sign (Craig et al. 2005a). One expects that commonly it will be the case that $\tilde{\kappa}_1 r > 0$ in situations where the solitons are of negative elevation. However, one can also imagine that $\tilde{\kappa}_1 r > 0$ could also hold for either negative or positive solitary wave elevations, in certain cases, as it depends as well on the sign of $\tilde{\kappa}_1$.

The coefficient $\tilde{\kappa}_1$ has a complicated but explicit expression in terms of k_0 and the parameters of the problem. In a forthcoming work, we plan to examine the relative signs of the Laplacian and the potential, and discuss the cases in which eigenvalues of the Schrödinger equation exist, and analyse further the character of the bound states associated with these eigenvalues. To complete the derivation, the equations for $\tilde{\mu}_1$ and $\tilde{\zeta}_1$ have the form

$$\varepsilon \partial_{\tau_1} \tilde{\mu}_1 = -\frac{1}{2}\omega_1^2(0)'' \partial_X^2 \tilde{\zeta}_1 + \tilde{\kappa}_4 \partial_X |v_1|^2 + c_0 \partial_X \tilde{\mu}_1, \tag{60}$$

$$\varepsilon \partial_{\tau_1} \tilde{\zeta}_1 = -\tilde{\mu}_1 + \tilde{\kappa}_3 |v_1|^2 + c_0 \partial_X \tilde{\zeta}_1, \tag{61}$$

from which we deduce that $\tilde{\mu}_1 \sim \partial_X \tilde{\zeta}_1 \sim |v_1|^2$.

5.6 Comparison with the rigid lid case

In order to quantify the differences between the rigid lid and free surface cases, we compare their ratios of nonlinearity to dispersion in the KdV regime. In the rigid lid case, this ratio is

$$R_L = \frac{3\left(\rho h_1^2 - \rho_1 h^2\right)}{h^2 h_1^2 (\rho_1 h_1 + \rho h)\sqrt{g(\rho - \rho_1)}}. \tag{62}$$

In the free surface configuration, it is defined by

$$R_S = \frac{24\kappa}{\omega^2(0)''''}, \tag{63}$$

where κ is given by (47) and

$$\begin{aligned} \frac{1}{24}\omega^2(0)'''' = &-\frac{gh^2}{3\rho^2}(\rho - \rho_1)(\rho h + 3\rho_1 h_1)a^-(0)^2 \\ &-\frac{gh}{3\rho^2}\sqrt{\rho_1(\rho - \rho_1)}\left(2\rho h^2 + 6\rho_1 h h_1 + 3\rho h_1^2\right)a^-(0)b^-(0) \\ &-\frac{g}{3\rho^2}\left(\rho^2 h_1^3 + \rho\rho_1 h^3 + 3\rho\rho_1 h h_1^2 + 3\rho_1^2 h^2 h_1\right)b^-(0)^2. \end{aligned}$$

Figure 5 shows the comparison between R_L and R_S as a function of the density ratio ρ_1/ρ, for different values of the depth ratio h_1/h. It is clear that there are significant differences between these two cases. First, we can see that R_L is always positive for $h_1/h > 1$, while R_S is always negative for $h_1/h < 1$. The ratio R_L changes sign only once in the range $\rho_1/\rho \in (0, 1)$ for $h_1/h < 1$. On the contrary, R_S changes sign once and then twice as h_1/h increases from 1.

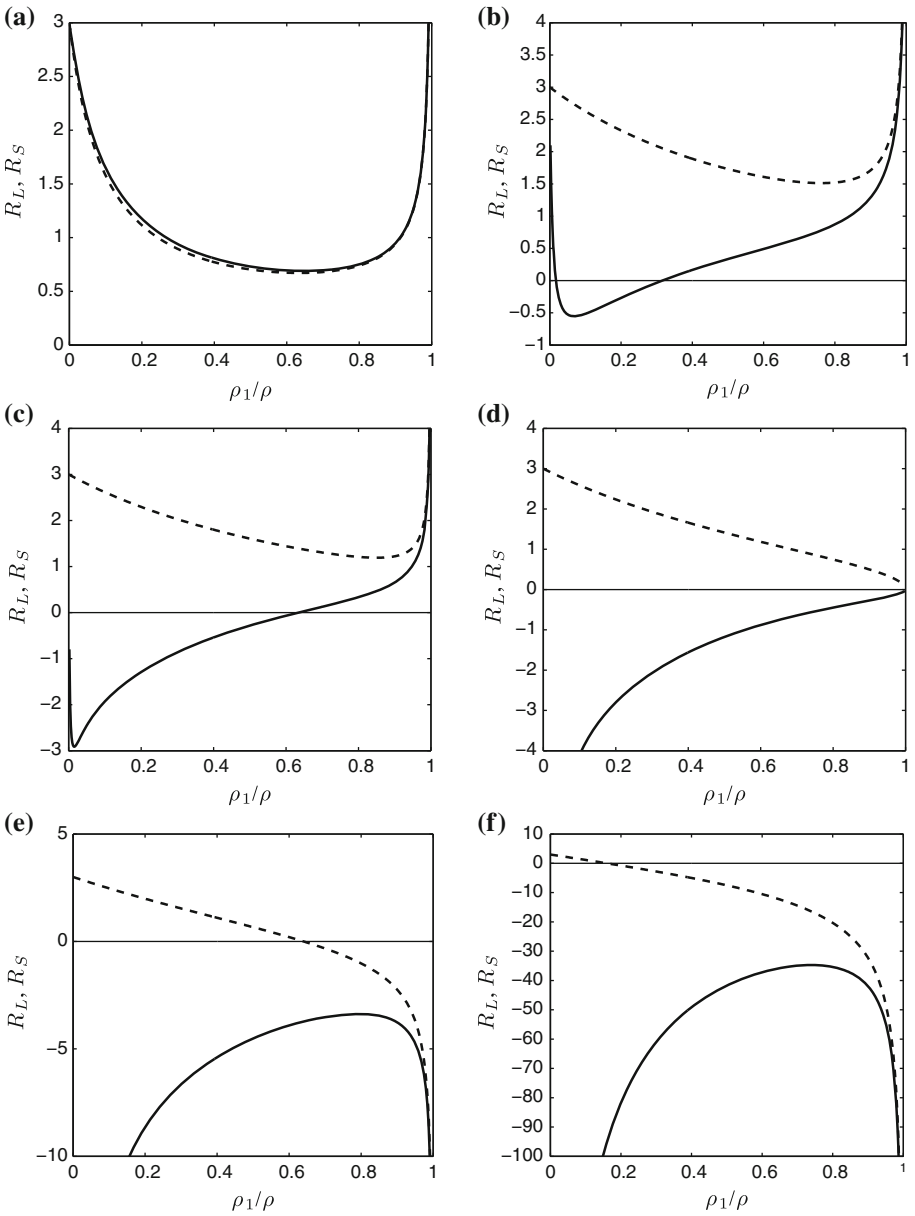

Fig. 5 Ratio of nonlinearity to dispersion for the interface in the KdV regime vs. density ratio ρ_1/ρ for (**a**) $h_1/h = 10$, (**b**) $h_1/h = 1.2$, (**c**) $h_1/h = 1.1$, (**d**) $h_1/h = 1$, (**e**) $h_1/h = 0.8$, (**f**) $h_1/h = 0.4$. The ratios R_L (rigid lid case) and R_S (free surface case) are represented in thick *dashed* and *solid lines* respectively

This property has important implications since the sign of the ratio determines the sign of solitary wave elevations. Benjamin (1966) found that, in the rigid lid case, the sign of R_L changes for $\rho_1/\rho = (h_1/h)^2$. We note that there is a widely varying difference between the sign of R_S and that of R_L for many parameter choices. Regarding the relative importance of nonlinearity and dispersion, it is observed that, for $\rho_1/\rho \simeq 0.9$ (which is close to realistic conditions), both $R_L, R_S \simeq O(1)$ in magnitude when $h_1/h \simeq 1$ and larger. This observation also holds true for a smaller density ratio, say $\rho_1/\rho \simeq 0.2$. As expected, the nonlinear effects prevail over the dispersive effects when h_1/h is small. We can nevertheless conclude that the Boussinesq and KdV regimes for the interface, in which dispersive and nonlinear effects are balanced, remain valid over a significant range of parameters.

6 Conclusions

This paper gives an asymptotic analysis of the coupling between the interface and the free surface of a two layer fluid, in a scaling regime in which the internal mode is treated as a long-wavelength nonlinear internal wave, while the surface mode is smaller and taken in a modulational regime. This is a physically realistic situation for certain cases of internal waves in the ocean, whose visible signature on the surface is a band of roughness which propagates at the same velocity as the internal wave. Using a perturbation theory based on an analogy with Hamiltonian mechanics, we have derived a coupled set of equations which describe this regime, in which the internal mode evolves according to an equation of KdV type, and the surface mode is propagated at the resonant group velocity, and is modulated according to a time-dependent linear Schrödinger equation. In the case of a soliton internal wave (when it is a wave of depression), this Schrödinger equation will often have bound states, leading to the phenomenon of trapped surface wave modes which propagate as the signature of the internal wave. It is proposed that this is a possible explanation for these bands of surface roughness mentioned earlier, which are associated with the presence of large amplitude internal waves.

Acknowledgments Walter Craig is partially supported by the Canada Research Chairs Program and NSERC through grant number 238452–06. Philippe Guyenne acknowledges support from the NSF through grant numbers DMS–0625931 and DMS–0920850. Catherine Sulem is partially supported by NSERC through grant number 46179–05.

Appendix

We present here a recursion formula for the higher-order terms in the Taylor series expansion for $G^{(m)}_{j\ell}(\eta, \eta_1)$. We distinguish two cases. The first is the special case where $m = (m_0, 0)$ or $(0, m_1)$, and the second is the more general case, where $m = (m_0, m_1)$ where neither m_0, $m_1 = 0$. In the first case, let $m = (m_0, 0)$. Then we can read from the matrix Eqs. 11, using 30, 31, 32 and 33, the following expressions for the matrix coefficients: the (11)-coefficient is

$$G_{11}^{(m_0,0)}(\eta) = \tfrac{1}{m_0!} D\eta^{m_0}(x) D^{m_0}\left(\tfrac{e^{-h_1 D}}{e^{h_1 D}-e^{-h_1 D}} + \tfrac{(-1)^{m_0} e^{h_1 D}}{e^{h_1 D}-e^{-h_1 D}}\right) + \sum_{\substack{p_0 \geq 1 \\ q_0+p_0=m_0 \\ q_1=0=p_1}} G_{11}^{(q_0,0)}(\eta) \frac{1}{p_0!} \eta^{p_0}(x) D^{p_0}\left(\frac{e^{-h_1 D}}{e^{h_1 D}-e^{-h_1 D}} + \frac{(-1)^{p_0+1} e^{h_1 D}}{e^{h_1 D}-e^{-h_1 D}}\right), \quad (64)$$

the (21)-coefficient is

$$G_{21}^{(m_0,0)}(\eta) = \sum_{\substack{p_0 \geq 1 \\ q_0+p_0=m_0 \\ q_1=0=p_1}} G_{21}^{(q_0,0)}(\eta) \frac{1}{p_0!} \eta^{p_0}(x) D^{p_0} \left(\frac{e^{-h_1 D}}{e^{h_1 D} - e^{-h_1 D}} + \frac{(-1)^{p_0+1} e^{h_1 D}}{e^{h_1 D} - e^{-h_1 D}} \right), \tag{65}$$

the (12)-coefficient is

$$\begin{aligned} G_{12}^{(m_0,0)}(\eta) &= -\tfrac{1}{m_0!} D\eta^{m_0}(x) D^{m_0} \left(\tfrac{1}{e^{h_1 D} - e^{-h_1 D}} + \tfrac{(-1)^{m_0}}{e^{h_1 D} - e^{-h_1 D}} \right) \\ &\quad - \sum_{\substack{p_0 \geq 1 \\ q_0+p_0=m_0 \\ q_1=0=p_1}} G_{11}^{(q_0,0)}(\eta) \frac{1}{p_0!} \eta^{p_0}(x) D^{p_0} \left(\frac{1}{e^{h_1 D} - e^{-h_1 D}} + \frac{(-1)^{p_0+1}}{e^{h_1 D} - e^{-h_1 D}} \right), \end{aligned} \tag{66}$$

and the (22)-coefficient is

$$G_{22}^{(m_0,0)}(\eta) = - \sum_{\substack{p_0 \geq 1 \\ q_0+p_0=m_0 \\ q_1=0=p_1}} G_{21}^{(q_0,0)}(\eta) \frac{1}{p_0!} \eta^{p_0}(x) D^{p_0} \left(\frac{1}{e^{h_1 D} - e^{-h_1 D}} + \frac{(-1)^{p_0+1}}{e^{h_1 D} - e^{-h_1 D}} \right). \tag{67}$$

A recursive computation of $G_{j\ell}^{(m_0,0)}(\eta)$ can be based upon formula (64) for $G_{11}^{(m_0,0)}(\eta), m_0 > 0$ and formula (65) for $G_{21}^{(m_0,0)}(\eta), m_0 > 0$. This is sufficient information in order to calculate $G_{12}^{(m_0,0)}(\eta)$ and $G_{22}^{(m_0,0)}(\eta)$ from respectively (66) and (67).

It is a general fact that

$$G_{j\ell}^{(m_0,m_1)}(\eta, \eta_1) = G_{\ell j}^{(m_1,m_0)}(-\eta_1, -\eta) \tag{68}$$

which allows us to deduce the form of $G_{j\ell}^{(0,m_1)}(\eta_1)$, with $j, \ell = 1, 2$ from the above expressions. As well, each matrix operator $G_{j\ell}^{(m)}$ is self adjoint, which is not necessarily self-evident from the above formulae. Thus in particular $\left(G_{12}^{(m)}\right)^* = G_{21}^{(m)}$. Therefore, the latter can be obtained from (66), which itself depends upon the recursion (64) alone.

The second case consists of those multi indices $m = (m_0, m_1)$ where neither m_0 nor m_1 vanish. The m-order terms on the right-hand side of the relation (11) are zero, as is seen in (32, 33). Working as in the first case, we find an expression for the (11)-coefficient to be

$$\begin{aligned} G_{11}^{(m_0,m_1)}(\eta, \eta_1) &= \sum_{\substack{1 \leq p_0 \leq m_0 \\ q_0+p_0=m_0 \\ p_1=0}} G_{11}^{(q_0,m_1)}(\eta, \eta_1) \frac{1}{p_0!} \eta^{p_0}(x) D^{p_0} \left(\frac{e^{-h_1 D}}{e^{h_1 D} - e^{-h_1 D}} + \frac{(-1)^{p_0+1} e^{h_1 D}}{e^{h_1 D} - e^{-h_1 D}} \right) \\ &\quad + \sum_{\substack{p_0=0 \\ 1 \leq p_1 \leq m_1 \\ q_1+p_1=m_1}} G_{12}^{(m_0,q_1)}(\eta, \eta_1) \frac{1}{p_1!} \eta_1^{p_1}(x) D^{p_1} \left(\frac{1}{e^{h_1 D} - e^{-h_1 D}} + \frac{(-1)^{p_1+1}}{e^{h_1 D} - e^{-h_1 D}} \right). \end{aligned}$$

The (21)-coefficient is

$$\begin{aligned} G_{21}^{(m_0,m_1)}(\eta, \eta_1) &= \sum_{\substack{1 \leq p_0 \leq m_0 \\ q_0+p_0=m_0 \\ p_1=0}} G_{21}^{(q_0,m_1)}(\eta, \eta_1) \frac{1}{p_0!} \eta^{p_0}(x) D^{p_0} \left(\frac{e^{-h_1 D}}{e^{h_1 D} - e^{-h_1 D}} + \frac{(-1)^{p_0+1} e^{h_1 D}}{e^{h_1 D} - e^{-h_1 D}} \right) \\ &\quad + \sum_{\substack{p_0=0 \\ 1 \leq p_1 \leq m_1 \\ q_1+p_1=m_1}} G_{22}^{(m_0,q_1)}(\eta, \eta_1) \frac{1}{p_1!} \eta_1^{p_1}(x) D^{p_1} \left(\frac{1}{e^{h_1 D} - e^{-h_1 D}} + \frac{(-1)^{p_1+1}}{e^{h_1 D} - e^{-h_1 D}} \right). \end{aligned}$$

The (12)-coefficient is the operator

$$G_{12}^{(m_0,m_1)}(\eta,\eta_1) = -\sum_{\substack{1\le p_0\le m_0\\ q_0+p_0=m_0\\ p_1=0}} G_{11}^{(q_0,m_1)}(\eta,\eta_1)\frac{1}{p_0!}\eta^{p_0}(x)D^{p_0}\left(\frac{1}{e^{h_1D}-e^{-h_1D}}+\frac{(-1)^{p_0+1}}{e^{h_1D}-e^{-h_1D}}\right)$$
$$-\sum_{\substack{p_0=0\\ 1\le p_1\le m_1\\ q_1+p_1=m_1}} G_{12}^{(m_0,q_1)}(\eta,\eta_1)\frac{1}{p_1!}\eta_1^{p_1}(x)D^{p_1}\left(\frac{e^{h_1D}}{e^{h_1D}-e^{-h_1D}}+\frac{(-1)^{p_1+1}e^{-h_1D}}{e^{h_1D}-e^{-h_1D}}\right).$$

Finally, the (22)-coefficient is

$$G_{22}^{(m_0,m_1)}(\eta,\eta_1) = -\sum_{\substack{1\le p_0\le m_0\\ q_0+p_0=m_0\\ p_1=0}} G_{21}^{(q_0,m_1)}(\eta,\eta_1)\frac{1}{p_0!}\eta^{p_0}(x)D^{p_0}\left(\frac{1}{e^{h_1D}-e^{-h_1D}}+\frac{(-1)^{p_0+1}}{e^{h_1D}-e^{-h_1D}}\right)$$
$$-\sum_{\substack{p_0=0\\ 1\le p_1\le m_1\\ q_1+p_1=m_1}} G_{22}^{(m_0,q_1)}(\eta,\eta_1)\frac{1}{p_1!}\eta_1^{p_1}(x)D^{p_1}\left(\frac{e^{h_1D}}{e^{h_1D}-e^{-h_1D}}+\frac{(-1)^{p_1+1}e^{-h_1D}}{e^{h_1D}-e^{-h_1D}}\right).$$

References

Benjamin TB (1966) Internal waves of finite amplitude and permanent form. J Fluid Mech 25:241–270

Benjamin TB (1967) Internal waves of permanent form of great depth. J Fluid Mech 29:559–592

Benjamin TB, Bridges TJ (1997) Reappraisal of the Kelvin-Helmholtz problem. I. Hamiltonian structure. J Fluid Mech 333:301–325

Bona JL, Lannes D, Saut J-C (2008) Asymptotic models for internal waves. J Math Pures Appl 89:538–566

Choi W, Camassa R (1999) Fully nonlinear internal waves in a two-fluid system. J Fluid Mech 396:1–36

Coifman R, Meyer Y (1985) Nonlinear harmonic analysis and analytic dependence. Pseudodifferential operators and applications (Notre Dame, 1984), 71–78. Proceedings of Symposia in Pure Mathematics, 43. American Mathematical Society, Providence, RI

Colin T, Lannes D (2001) Long-wave short-wave resonance for nonlinear geometric optics. Duke Math J 107:351–419

Craig W, Groves M (1994) Hamiltonian long-wave approximations to the water-wave problem. Wave Motion 19:367–389

Craig W, Groves M (2000) Normal forms for waves in fluid interfaces. Wave Motion 31:21–41

Craig W, Guyenne P, Kalisch H (2004) A new model for large amplitude long internal waves. C R Mecanique 332:525–530

Craig W, Guyenne P, Kalisch H (2005a) Hamiltonian long-wave expansions for free surfaces and interfaces. Comm Pure Appl Math 58:1587–1641

Craig W, Guyenne P, Nicholls DP, Sulem C (2005b) Hamiltonian long-wave expansions for water waves over a rough bottom. Proc R Soc A 461:839–873

Craig W, Guyenne P, Sulem C (2010) A Hamiltonian approach to nonlinear modulation of surface water waves. Wave Motion. doi:10.1016/j.wavemoti.2010.04.002

Craig W, Nicholls DP (2002) Traveling gravity water waves in two and three dimensions. Eur J Mech B/Fluids 21:615–641

Craig W, Sulem C (1993) Numerical simulation of gravity waves. J Comput Phys 108:73–83

Dias F, Ilichev A (2001) Interfacial waves with free-surface boundary conditions: an approach via a model equation. Physica D 150:278–300

Duchêne V (2009) Asymptotic shallow water models for internal waves in a two-fluid system with a free surface. Preprint, ArXiv:0906.0839v1

Fazioli C, Nicholls DP (2008) Parametric analyticity of functional variations of Dirichlet-Neumann operators. Diff Int Eq 21:541–574

Gear J, Grimshaw R (1984) Weak and strong interactions between internal solitary waves. Stud Appl Math 70:235–258

Global Ocean Associates (2002) Contribution to *An atlas of internal solitary waves: The Andaman Sea*. Report prepared for the Office of Naval Research, code 322PO

Hashizume Y (1980) Interaction between short surface waves and long internal waves. J Phys Soc Japan 48:631–638

Landau LD, Lifshitz EM (1960) Mechanics. Pergamon Press, Oxford-London-New York-Paris

Osborne AR, Burch TL (1980) Internal solitons in the Andaman Sea. Science 208:451

Parau E, Dias F (2001) Interfacial periodic waves of permanent form with free-surface boundary conditions. J Fluid Mech 437:325–336

Peters AD, Stoker JJ (1960) Solitary waves in liquids having non-constant density. Comm Pure Appl Math 13:115–164

Zakharov VE (1968) Stability of periodic waves of finite amplitude on the surface of a deep fluid. J Appl Mech Tech Phys 9:190–194